JOURNAL OF MATERIALS SCIENCE 37 (2002) 1895–1905

Effect of stabilizer on fatigue resistance of a polyoxymethylene (acetal) copolymer

E. A. SHOWAIB, M. G. WYZGOSKI
Delphi Research Labs, Delphi Automotive Systems, 51786 Shelby Parkway, Shelby Township, MI 48315, USA
E-mail: michael.g.wyzgoski@delphiauto.com

Acetal is known for its fatigue resistance, however, it is also susceptible to degradation at high temperatures. Commercial resins therefore contain complex stabilizer systems that, although present in relatively small amounts, provide thermal stability both for processing and subsequent in-service aging. The present study was undertaken to determine how sensitive the fatigue resistance of an acetal copolymer was to changes in stabilizer concentration. Blends containing a series of increasing stabilizer levels were investigated and compared to the commercial material. Fatigue resistance was assessed using accelerated fatigue crack propagation rate measurements for injection molded plaques. Results demonstrate that the fatigue resistance is dependent upon the amount of stabilizer and in fact suggest that a critical level of stabilizer is needed to provide adequate fatigue resistance in the molded part. It is also shown that room temperature aging further aggravates the poor fatigue resistance of samples with low stabilizer levels. Moreover, the results from this study demonstrate that the varying concentrations of heat stabilizer affect even short term mechanical properties such as tensile modulus, strength, and elongation to fail. In addition, fracture toughness tests clearly distinguish the various materials. The short term mechanical tests provide added support that a critical concentration of stabilizer exists.

1. Introduction

Acetal is the common name for polyoxymethylene (POM). The latter is more structurally descriptive because the repeat unit for acetal is $(CH_2{-}O)_n$. Commercially there are two types of acetal: (a) homopolymers (Delrin) introduced by E. I. duPont and (b) copolymers (Celcon) made by Hoechst Celanese (now Ticona). The main challenge to the commercialization of this material was the different modes of degradation that had to be overcome. Some of these modes are: unzipping from the chain ends, oxidation followed by depolymerization, acidic attack on the acetal chain, and thermal degradation [1]. Therefore, commercial acetal contains additives that prevent the modes of degradation or enhance the acetal's resistance to such modes. The presence of these stabilizer additives, although in relatively low concentrations, allows the acetal to be processed in the usual high temperature melt forming methods such as injection molding and extrusion. An excellent review of the stabilization of polyacetals, both homopolymers and copolymers, was published by Stohler and Berger [2].

Acetal, being a highly crystalline material, is widely used in applications requiring good chemical resistance and wear resistance. It is also known for its excellent fatigue resistance. In fact, some authors have indicated that it is the most fatigue resistant engineering plastic available [3]. Others have noted that both crack initiation and propagation should be considered in ranking polymers and in some cases, nylons may be more resistant to the initiation of a fatigue crack [4]. Ironically, although acetals are highly fatigue resistant, they also exhibit relatively brittle behavior. In fact, it is often difficult to generate stable fatigue crack growth without inducing premature fracture [3]. Acetal fatigue is also known to involve both thermal induced and mechanical failure mechanisms [5], and significant hysteretic heating can occur even in bending or flexural fatigue [6, 7]. The situation is further complicated by indications that even the mechanical fatigue failure of acetal may involve chemical degradation mechanisms such as chain scission [4, 8]. Physical changes, such as volume increases, induced by fatigue loading, even in the low stress mechanically dominated region, have also been reported [9]. Others have shown through fracture toughness measurements that the acetal matrix is damaged by fatigue stressing, even before any noticeable cracking is evident [4]. The role of molecular weight, spherulitic morphology and rubber toughening have also been described in some of these same articles [4, 8] and others [10]. The extensive literature on acetal suggests that the fatigue resistance of any given acetal sample may depend on how well the material had been stabilized and of course how well the stabilizer package survives the thermal history required to prepare the finished part.

The present study was therefore undertaken to determine the effect of the concentration of stabilizer on the fatigue behavior of acetal. In addition to fatigue resistance, the short term mechanical performance was also assessed by tensile property and fracture toughness measurements.

2. Experimental procedure

2.1. Materials

The material employed in this study is a commercially available acetal copolymer manufactured by Ticona and designated as Celcon M25. The M25 stands for the melt flow rate or melt index which for this resin is 2.5 grams per 10 minutes, as stated in ASTM standard D1238. Ticona also kindly provided experimental materials by extrusion compounding various concentrations of the stabilizer package into the M25 base resin. The identity of the stabilizer chemistry is proprietary as is the exact concentration used for the commercial product. However the stabilizer concentration was reported in terms of the relative amount in comparison to the standard M25 material. Taking the latter as 100%, the specially prepared blends were at 20, 40, 60, 80, 100, and 120% of that amount and are designated simply as B#1 through B#6. Note that the specially prepared blend, B#5, at 100% should therefore be similar to the original M25 material in terms of stabilizer concentration. It may not be identical since it was prepared off line as a smaller batch. Table I summarizes the materials.

2.2. Sample preparation

The acetal blends were supplied in the form of pellets, which were molded using an Engel, Model-830, injection molding machine with the conditions listed in Table II. Test plaques were prepared having dimensions 50.8 mm × 203.2 mm with a thickness of 3.2 mm. As shown in Fig. 1, the injection molding gate was in the 50.8 mm side of the plaque thus the melt flow direction is parallel to the long dimension.

TABLE I Material designations and percentage of stabilizer

Material	Percentage of stabilizer relative to M25	Note
B#1	20%	Special product
B#2	40%	Special product
B#3	60%	Special product
B#4	80%	Special product
B#5	100%	Special product
M25	100%	Commercial
B#6	120%	Special product

B#5 and M25 both have the same amount of stabilizer but they are from different lots.

TABLE II Molding conditions

Zone 1 temp.	221°C	Inject time	19.9 sec
Zone 2 temp.	215°C	Inject hold time	20.0 sec
Zone 3 temp.	215°C	Cool cure time	43.0 sec
Nozzle temp.	221°C	Mold temp.	85°C
Open cycle Time	2.0 sec	Injection pressure	98 MPa

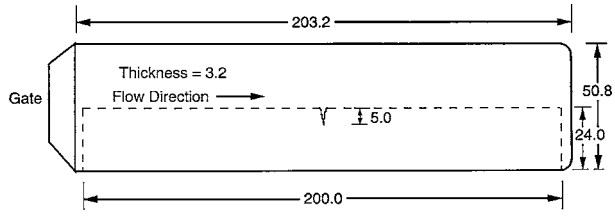

Figure 1 Schematic view of injection molded plaque and Single Edge Notch (SEN) sample used for fatigue crack growth measurements.

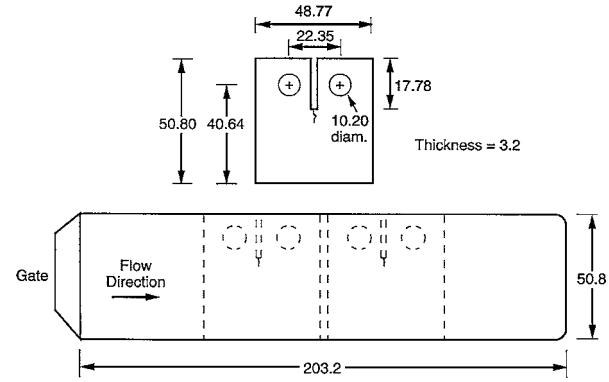

Figure 2 Schematic view of injection molded plaque and Compact Tension (CT) sample used for selected fatigue crack growth measurements.

2.2.1. Fatigue specimens

Preliminary fatigue crack growth experiments were performed using a compact tension (CT) sample geometry, following earlier work for nylon materials [11]. The shape, dimensions, and the locations of the CT specimens in the molded plaque are shown in Fig. 2.

Significant difficulty was encountered owing to the instability of precracks in the acetal material. The results did demonstrate that no anisotropy existed in the measured fatigue crack growth rates for these plaques. However, it was established that the samples precracked perpendicular to the melt flow direction were more stable in terms of initiating fatigue cracks. Subsequently it was decided to switch to a single edge notch (SEN) geometry. The latter specimen was chosen because it was expected to provide a more stable propagation of the fatigue crack compared to the CT geometry. Also because the crack propagation speed is much higher than that in the CT sample, the test time will be shorter in a SEN than in a CT specimen.

Fig. 1 shows the SEN specimen shape and dimensions in relation to the molded plaque. The notch was necessarily introduced in the direction perpendicular to the melt flow direction. As noted above, this orientation of the sample takes advantage of any molecular or morphological alignment near the surface of the injection molded plaque which had appeared to stabilize the initiation and growth of the fatigue crack in the tests with CT specimens.

Precracks were first saw cut to a depth of 3.5 mm and then razor cut an additional 1.5 mm. For the latter, a special computerized notching machine was designed and used to introduce the razor precrack in the test specimen by driving the blade into the sample at a controlled speed of 0.01 mm per sec. The precrack was cut perpendicular to the flow direction and close to the center of the plaques (side away from the molded edge).

Fatigue tests were conducted under two different temperatures, 25°C and 60°C, using a servo-hydraulic closed-loop testing machine (Instron Model 8500). The test frequency was set at one hertz to avoid hysteretic heating. A sinusoidal wave form was used under load control conditions with an R ratio (minimum to maximum load ratio) equal to 0.1. The maximum nominal stress was 14.1 MPa at room temperature and 12.2 MPa for the test conducted at 60°C. The maximum stress at room temperature was chosen based upon results which were published by Hertzberg *et al*. [3], in which it was mentioned that the lower ΔK at which they were able to propagate a stable fatigue crack was approximately 2 MPa* $m^{0.5}$. Subsequently however, at 60°C, we found it possible to propagate the crack at a lower ΔK of 1.5 MPa* $m^{0.5}$.

2.2.2. Tensile properties

The specimens used for measuring tensile properties were cut in accordance with ASTM Standard D 638M–93, Standard Test Method for Tensile Properties of Plastics, Type V. The specimens were cut parallel to the flow direction. The test conditions were: strain rate = 0.1/s, 23°C, with an extensometer gage length of 7.5 mm.

2.2.3. Fracture toughness specimens

Fracture toughness, K_{IC}, was also measured using the compact tension, CT, sample geometry in accordance with ASTM Standard E399. As mentioned earlier, and as shown in Fig. 2, the CT samples were cut from the molded plaques so that the crack would be propagating in the direction perpendicular to the melt flow direction.

2.3. Fatigue crack propagation rate measurements

The fatigue crack propagation was monitored using a time-elapsed video recorder and a special lens (Questar QM1) with which it was possible to get a high magnification (100 X) on the screen while the video camera was far from the test specimen (out of the environmental chamber). The crack propagation measurements were made by playing the video tape after the end of the test and employing a video analyzer/densitometer to observe the crack position. Details of this technique were previously published for nylon fatigue studies [11]. Subsequent fractography demonstrated that the optically observed crack position was an accurate assessment of the interior crack position for the acetal samples.

3. Results and discussion

3.1. Initiation of stable fatigue cracks

The most common problem facing any study conducted on fatigue crack propagation of acetal or other nominally brittle materials is to initiate a stable crack [3, 12]. This difficulty was encountered in the present study especially during the room temperature tests. For example, in some specimens, a fatigue crack did not propagate in stable fashion even though a well defined damage zone initiated at the notch. The specimen could take days to initiate a crack and then, suddenly, the specimen fractured catastrophically without generating any stable fatigue crack propagation. It was believed that the reason for this erratic behavior is the relatively uncontrolled residual stress from notching and the thermal history of each sample. Therefore several methods were tried to minimize the variation between samples. For example, the notching procedure discussed above was designed to minimize variations in residual stress. Another method was to preheat the test specimen after notching for 48 hr at 80°C to relax the residual stresses. These changes lead to improvements in the stability and reproducibility of the crack propagation experiments, however, they did not eliminate the problem completely in room temperature tests. Fortunately it was found that the instability problems did disappear with the higher temperature testing at 60°C.

Thus the following procedure was adopted. For the testing at high temperature, notching was performed immediately prior to starting the fatigue test. The oscillating load was applied one hour after the notched sample was mounted in the test frame. This hour allowed the test specimen and the environmental chamber to reach the steady state condition. However, for the room temperature tests, the prenotched sample was first subjected to a low oscillating load level at 60°C to preinitiate a stable fatigue crack. By this method it was possible to stabilize the crack initiation and propagation and to get reproducible results.

3.2. Fatigue crack propagation

A typical crack propagation data set is shown in Fig. 3. The method for fitting the crack length versus number of cycles that was developed by one of the authors (ES) [13] has been employed in this study with only a small change to fit these materials. This method has also

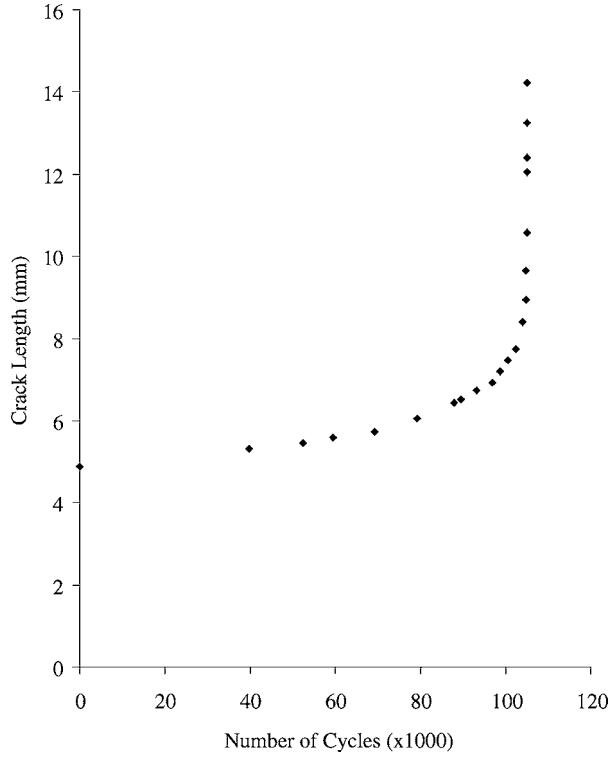

Figure 3 Crack length versus number of fatigue cycles for Celcon M-25 resin at room temperature and at a frequency of 1 Hz with $R = 0.1$.

been employed for many other materials [14–16]. The crack length data are plotted versus the difference between N_f (total number of cycles to failure) and N (the number of cycles at which the crack was measured), or (N_f-N). For example, the crack length measurements in Fig. 3 were redrawn versus N_f-N while also changing the domain from a normal to a semilogarithmic scale as shown in Fig. 4a. One can see that the data are fit very well by a straight line. In some cases, a log-log relationship is needed to completely fit all the data or two different straight line regimes may be noted [13–15]. The equation of the straight line in the semilogarithmic plot is:

$$\mathbf{a}_n = -C_1 * \log(N_f\text{-}N) + C_2$$

Where $\mathbf{a}_n$ is the crack length at N number of cycles and both C_1 and C_2 are constants for the material at this loading condition and sample configuration. C_1 is the straight line slope and C_2 is the intersection with the crack length axis. The result of the fitting is shown in Fig. 4b with the original crack propagation measurements. C_1 has been observed to be a material constant independent of loading conditions, for example different R ratios and load levels have no effect on C_1 [16].

During the course of this study, it was noted that a transition does occur at higher ΔK values where the fatigue crack accelerated greatly just prior to sample rupture. The fatigue crack growth rate data at these higher ΔK levels deviated from the relationship shown in Fig. 4. Moreover, in this regime an apparent change in crack propagation mechanism also occurred. The latter was substantiated by fractography observations. At lower ΔK the surface was patchy while at higher ΔK the texture was more drawn out, very similar to the observations of Bretz *et al.* for nylon (See Fig. 3 in Ref. 8). Because of the complete change in the morphology of the fracture surface at the higher ΔK level, the latter region of relatively high speed, yet stable, tearing was avoided in representing the fatigue crack growth data.

One can substitute the above equation into the equation of the stress intensity factor to get a mathematical relation between the stress intensity and the crack speed. However this relation will be very complicated; therefore we chose here to follow the previous approach [11], using a polynomial curve fitting approach at a certain number of cycles to calculate a, da/dN, and ΔK. Applying this procedure for the data in Fig. 3 one obtains the da/dN versus ΔK relationship shown in Fig. 5

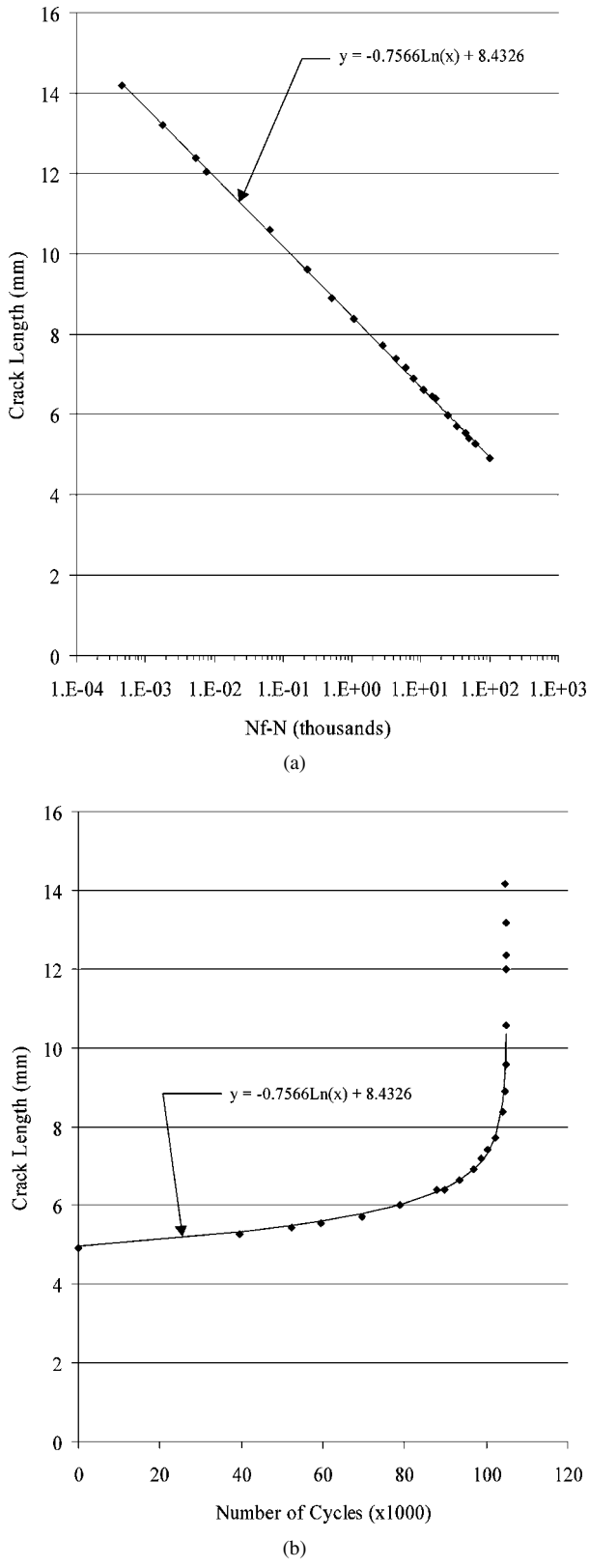

Figure 4 (a) Replot of data in Fig. 3 versus N_f-N on a semilogarithmic scale (b) Result of fitting equation being applied to the crack growth data for Celcon M-25.

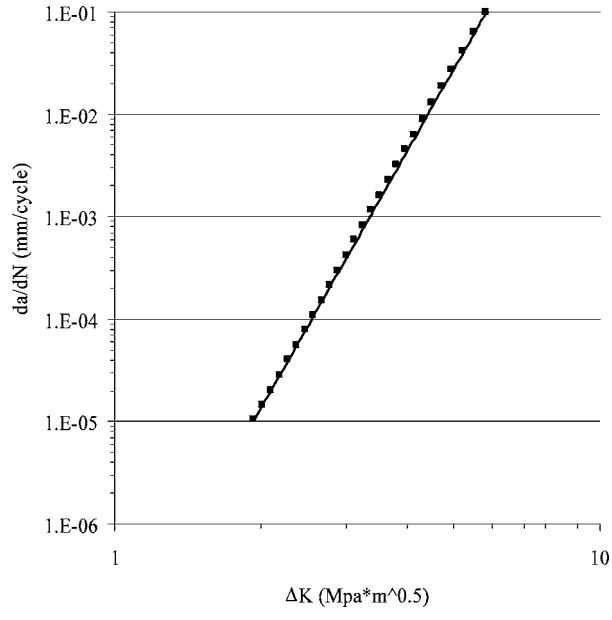

Figure 5 Paris Equation fit to the fatigue crack growth rate results for Celcon M-25 acetal.

which were fitted to a straight line in the logarithmic domain using the Paris Equation [17]:

$$da/dN = A * (\Delta K\hat{}m)$$

where A and m are treated as material constants. The equation for the stress intensity factor for the SEN geometry which was used in this study is [18]:

$$\Delta K = \sigma\sqrt{a}F\left(\frac{a}{w}\right)$$

where:

$$F(a/w) = 1.12 - 0.231(a/w) + 10.55((a/w)^2) \\ -21.71((a/w)^3) + 30.382((a/w)^4).$$

3.3. Effect of stabilizer on fatigue crack propagation

Implementing the above methodology to get the fatigue crack propagation rate as a function of the stress intensity factor range (ΔK), we were able to detect small differences between the different blends. Fig. 6 shows the da/dN versus ΔK relationships for the tests at 60 °C and Fig. 7 shows the relationships at room temperature. As mentioned earlier, the straight lines in Figs 6 and 7 are representative of the fatigue crack propagation rate data at the lower ΔK levels. From a first look at the above figures it is very difficult to distinguish between the different blends or to identify which blend is most resistant to fatigue crack propagation. In fact at higher ΔK levels it is possible to conclude that lower stabilizer levels improve the fatigue resistance (slower crack growth rates). The confusion exists because the slopes are not the same in all of the blends and in fact they

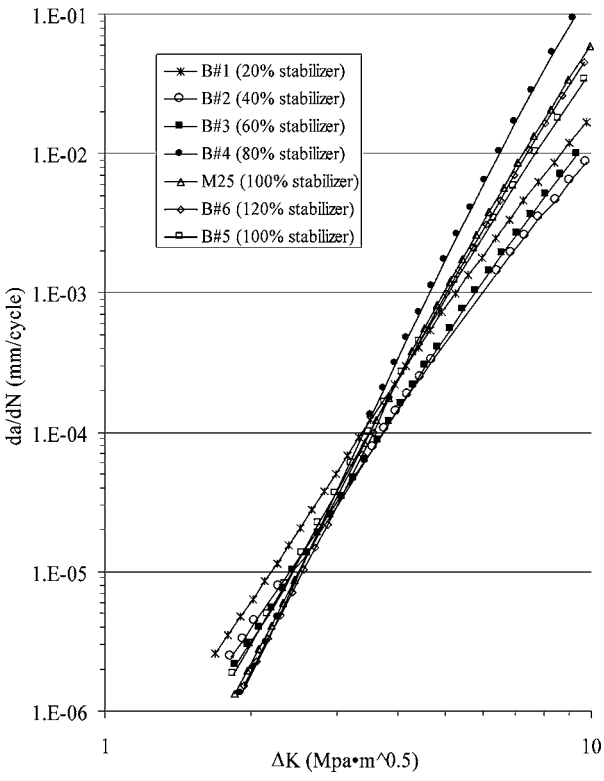

Figure 6 Fatigue crack growth rate measurements at 60°C for acetal containing various concentrations of stabilizer.

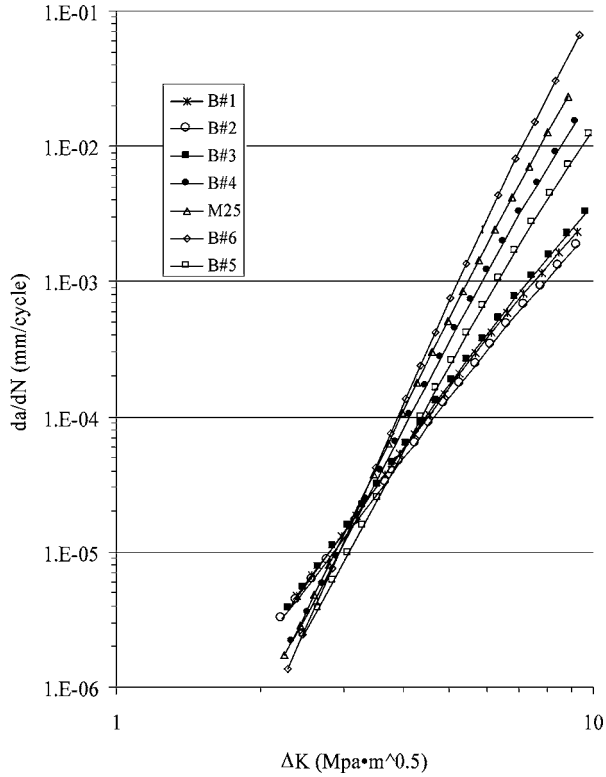

Figure 7 Fatigue crack growth rate measurements at 25°C for acetal containing various concentrations of stabilizer.

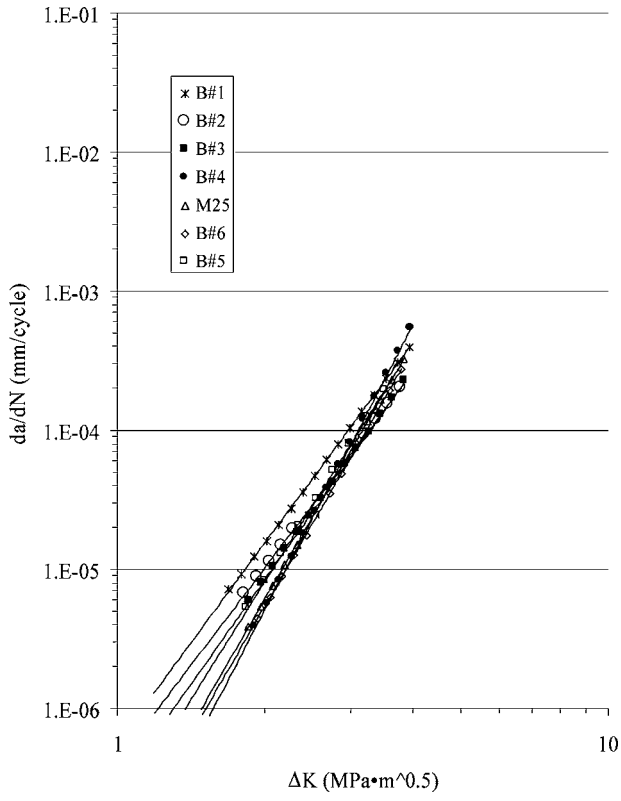

Figure 8 Extrapolation of fatigue crack growth rate measurements at 60°C for acetal blends at lower stress intensities.

intersect one another. To clarify the situation we therefore extrapolated the lower portion of the Paris equation plots to much lower ΔK as shown in Figs 8 and 9 for the two different temperatures. The lower stress intensities are believed to be more representative of fatigue conditions in actual parts and the crack propagation is

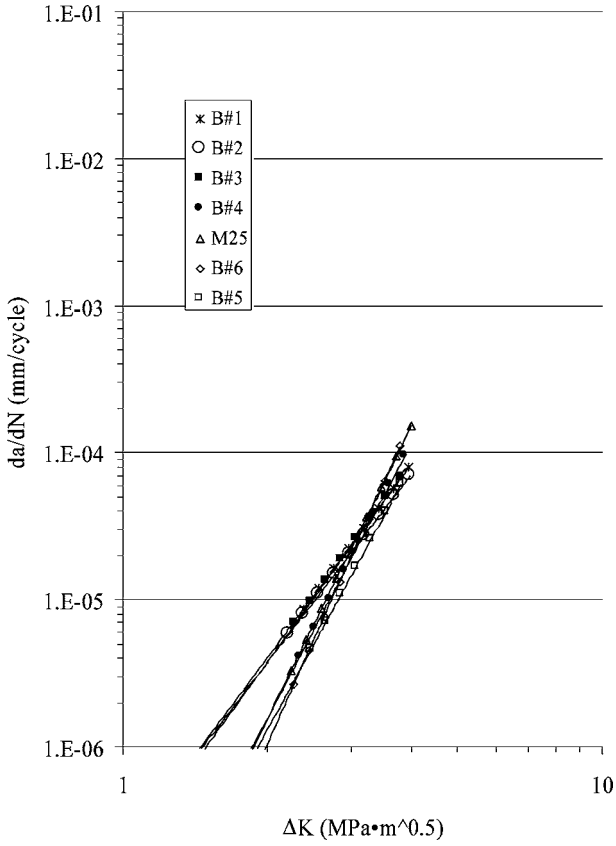

Figure 9 Extrapolation of fatigue crack growth rate measurements at 25°C for acetal blends to lower stress intensities.

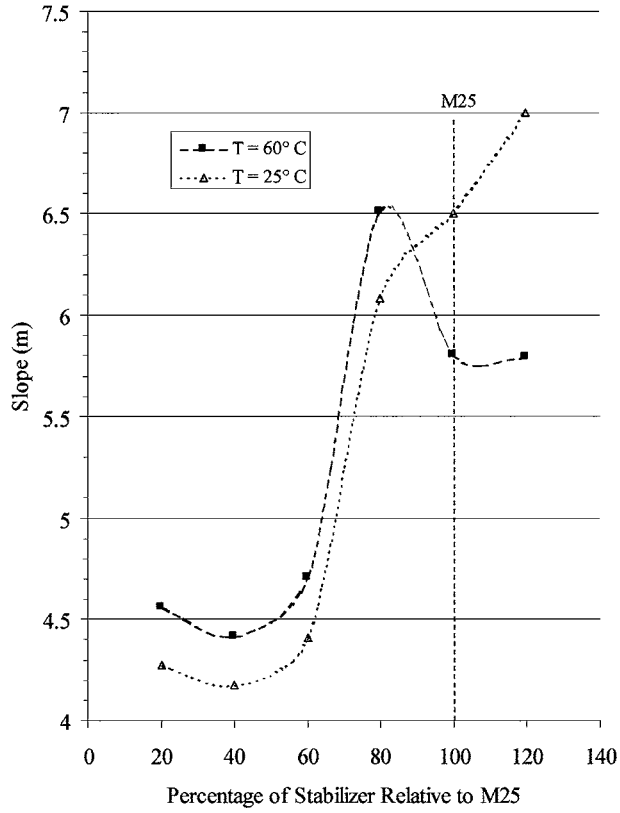

Figure 10 Slope of Paris Equation for acetal blends containing various concentrations of stabilizer.

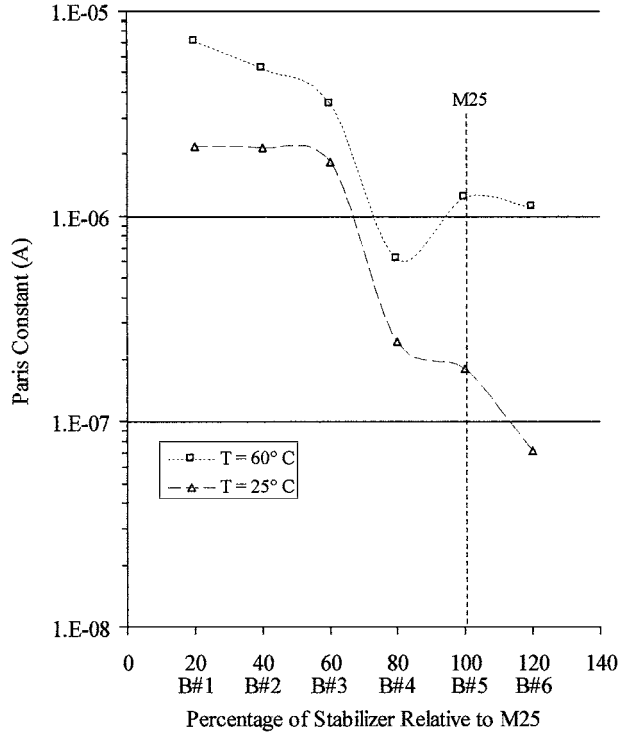

Figure 11 Paris Equation constants for acetal blends containing various concentrations of stabilizer.

less likely to be influenced by high speed ductile tearing mechanisms.

General speaking, the results in Figs 8 and 9 allow us to identify two different groupings in the materials; one having higher crack propagation rates (lower resistance to fatigue), and the other having lower crack speeds (improved resistance to fatigue). The first group consists of the blends that have a stabilizer content of 60% or lower (20%, 40%, 60%) while the other group is the blends that have 80% or more stabilizer (80%, 100%, 120%). This grouping of the data, especially for the room temperature testing, suggests that a critical concentration of stabilizer exists at 80% (relative to the amount which is used in the commercial acetal product M25) to insure excellent fatigue resistance of acetal.

The constants A and m of the Paris equation define quantitatively the fatigue resistance of each of the blends and thus are useful in understanding the fatigue crack propagation behavior. Figs 10 and 11 show the values of these constants for both room and high temperature tests at the different stabilizer levels. From Fig. 10 it is clear that the materials that have 60% or less of the additive, exhibit similar slopes, with m being close to 4 (4.3 to 4.7). Interestingly, it has been demonstrated mathematically that an m value of 4 is the expected value for nominally brittle materials [19]. Therefore, one might expect that these three blends would be more brittle than the other materials as will be discussed later. In contrast, the blends that have 80% or more stabilizer, relative to M25, show higher slopes.

The A and m values derived from the fatigue crack propagation rate data are often treated as material constants. However, their significance or interpretation is not always clear. In cases where m is relatively constant, the value of A can provide a convenient quantitative ranking of fatigue resistance, with lower A representing improved fatigue performance. Unfortunately, when both A and m are changing, as is the case for

the various acetal blends, the relative ranking of fatigue resistance is not obvious. In such a case, as was mentioned earlier, it is valuable to calculate an apparent fatigue lifetime for each of the blends. The lifetime is obtained from a numerical integration of the Paris equation using both A and m. One must first assume an initial or preexisting flaw (small crack) and a stress level. The results of such calculations for the acetal blends and the specific conditions assumed are shown in Fig. 12 for both room temperature and 60°C. These fatigue lifetimes are also reported in Table III along with the ratio between the room temperature and 60°C values.

In general from the results of the integration it is clear that there is a dramatic change in the lifetime between B#3 and B#4 (from 60% to 80% stabilizer). Note that at 25°C, for blends having 60% or lower of stabilizer the integrated lifetime is almost the same; while at 80% stabilizer, or higher, the integrated lifetime increases with increasing percentage of stabilizer. This result suggests that there may be added benefit to even higher concentrations of stabilizer in terms of extending the fatigue life of acetal parts. At 60°C the lifetime results indicate that there are still two groupings of results for low and high stabilizer levels, however, the latter appears to be independent of the level, i.e., there is not a continual increase with added stabilizer. By looking carefully at the ratio between the integrated lifetime at 25°C, and that at 60°C, as shown in Table III, one can see that the ratio for the first four blends (B#1, B#2, B#3, B#4) is about three. However, for M25 and B#6 the ratio is almost double that value.

An additional advantage of the lifetime calculation is that the dramatic effect of temperature on fatigue life becomes very evident. By increasing the temperature from 25 to 60°C the lifetime becomes one third or less than that at 25°C, as shown in Table III. This underscores the strong role of temperature in dictating the lifetime of parts in service and the need for component testing at high temperatures representative of use conditions.

TABLE III Integrated lifetimes versus temperature

Material	Percent stabilizer	Integrated life at 60°C (days)	Integrated life at 25°C (days)	Ratio of the life 25°C/60°C
B#1	20%	7.2	22.1	3.07
B#2	40%	8.0	23.1	2.87
B#3	60%	9.5	27.5	2.89
B#4	80%	27.2	81.4	2.99
M25, B#5	100%	18.8	110.0	5.85
B#6	120%	21.0	166.3	7.9

3.4. Tensile properties

Representative stress strain curves for each of the blends and the commercial acetal material are shown in Fig. 13. Typically four to six samples were run for each blend and standard deviations will be shown in subsequent plots. Fig. 13 suggests two groupings of the data: B#1, B#2 and B#3 in one group exhibiting higher modulus and strength but with lower strain at failure; and B#4, M25 (indistinguishable from B#5) and B#6 in a second group with higher strains to fail, yet lower modulus and strength. These differences are shown in detail in Figs 14–16. The strengths vary by only 10%, however a consistent trend is noted, especially considering the data scatter for each blend. In fact a precipitous drop is suggested between blends B#3and B#4 which

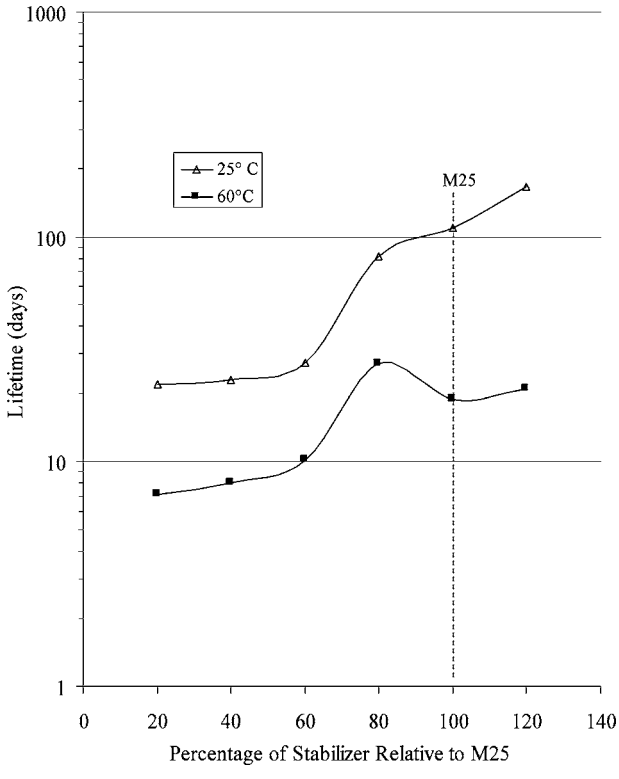

Figure 12 Apparent fatigue lifetimes at 25°C and 60°C for acetal blends containing various concentrations of stabilizer.

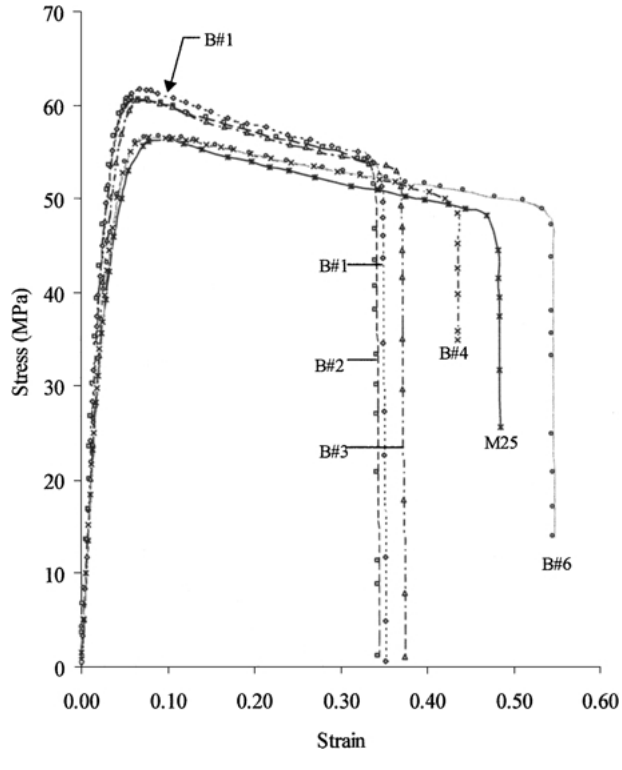

Figure 13 Stress – Strain behavior of acetal blends.

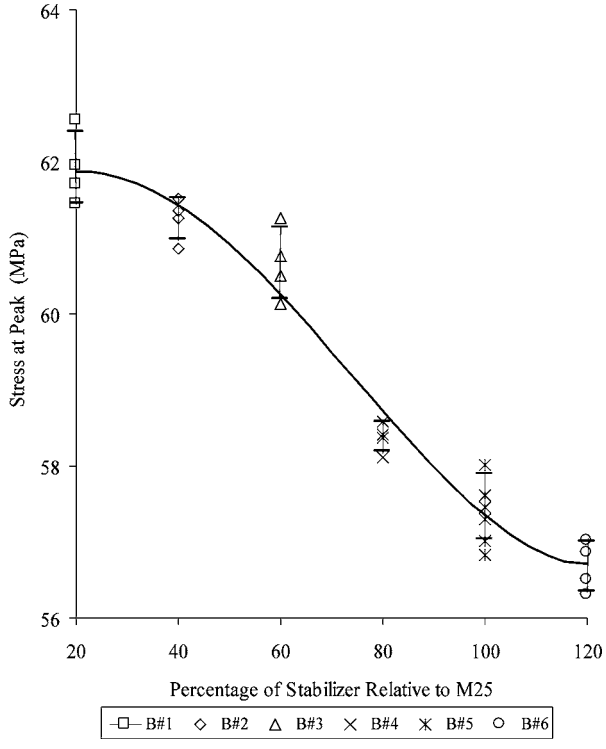

Figure 14 Tensile yield stress versus concentration of stabilizer for acetal blends.

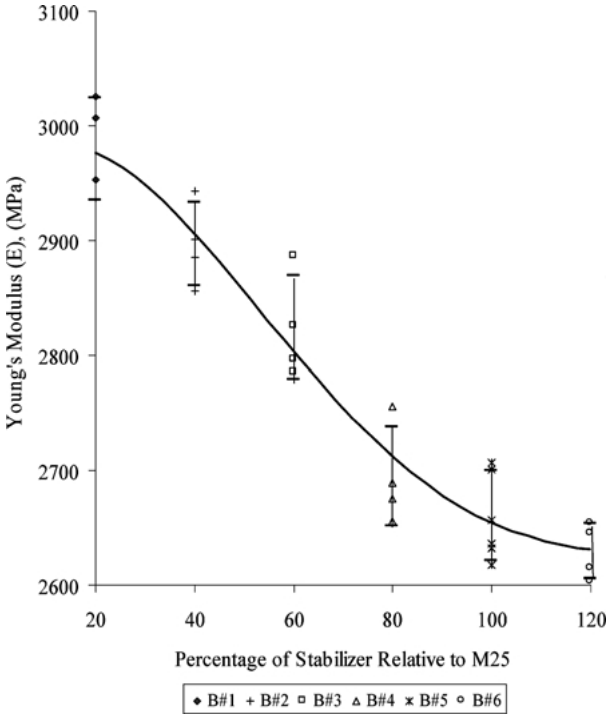

Figure 15 Tensile Modulus versus concentration of stabilizer for acetal blends.

may indicate a critical stabilizer level. The moduli decreases (Fig. 15) also suggest a leveling off beyond blend B#4. Similarly the maximum strain (Fig. 16) is relatively constant for blends B#1, B#2 and B#3, then increases dramatically at the higher levels. Although the commercial resin is well above the apparent critical level in stabilizer concentration, it also seems that even higher concentrations of stabilizer may be beneficial. Taken together, the tensile stress-strain results

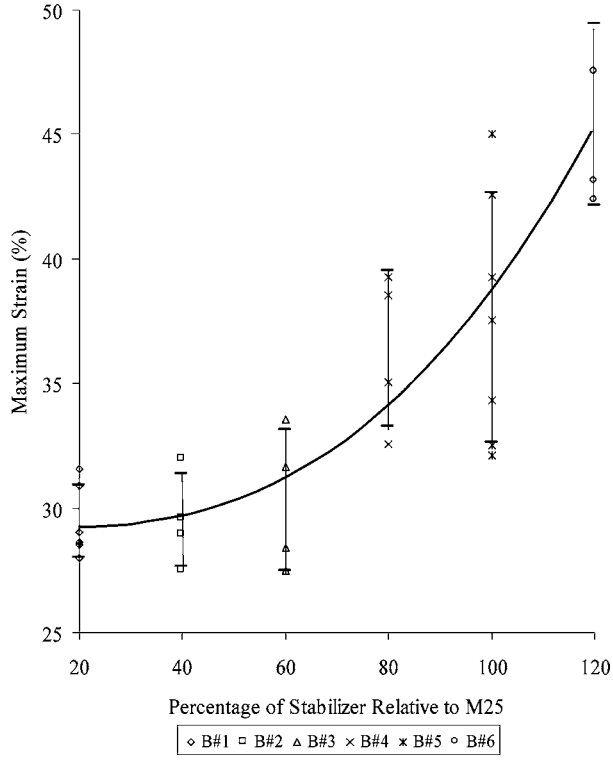

Figure 16 Maximum tensile strain versus concentration of stabilizer for acetal blends.

suggest that the blends with lower stabilizer levels are more prone to brittle behavior and fracture toughness measurements were pursued to further address this possibility.

3.5. Fracture toughness

Fracture toughness measurements require the use of relatively thick samples to insure that plane strain conditions exist at the crack tip so as to minimize the contributions of plasticity or yielding on the calculated K_{1c} values. The use of relatively thin, 3.2 mm, samples can be questioned, however, additional quantities of the blend materials were not available to mold thicker plaques. Fortunately the K_{1c} measurement procedure allows one to assess the validity of the measurement from the linearity of the load-displacement data. Fig. 17 demonstrates that for the blend B#1, the load-displacement curve for the compact tension sample is relatively linear up to the failure load. Similar curves were also observed for B#2 and B#3. The ASTM Standard quantifies the nonlinearity by using a 5% offset compliance to define a load, P_Q which is the intercept of the offset with the load-displacement trace. P_Q is then compared to the maximum load, P_M. The linearity requirement is that the difference is less than 10%. For blends B#1–B#3 the use of P_Q is valid, there is little difference between P_Q and P_M. However for blends with higher stabilizer levels, B#4–B#6, this was not the case as significant nonlinearity occurred. This is shown in Fig. 18 where B#1 and B# 5 are shown along with the indications of P_Q and P_M. Note that for blend B#5, P_Q is significantly less than P_M. The latter suggests that the use of maximum values is not valid

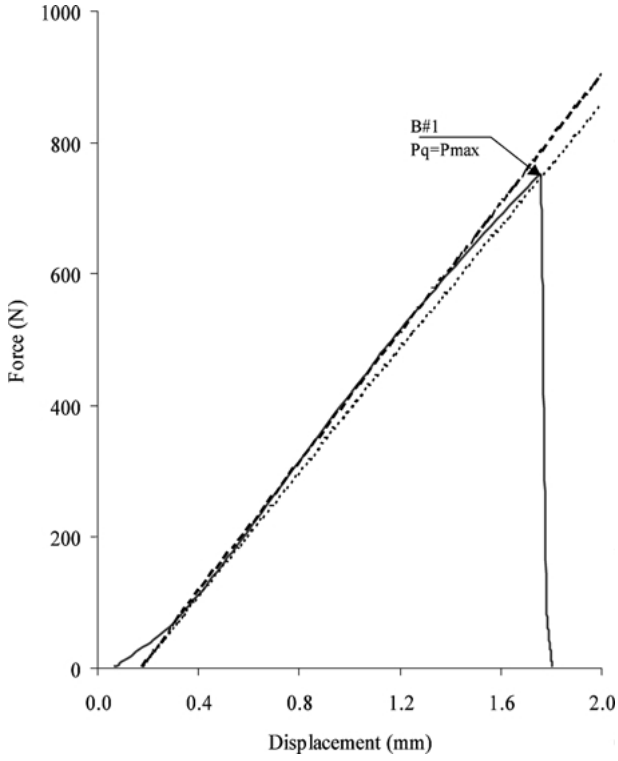

Figure 17 Force - Displacement trace during fracture toughness testing of acetal blend B#1. Note: P_Q and P_M are defined in the text.

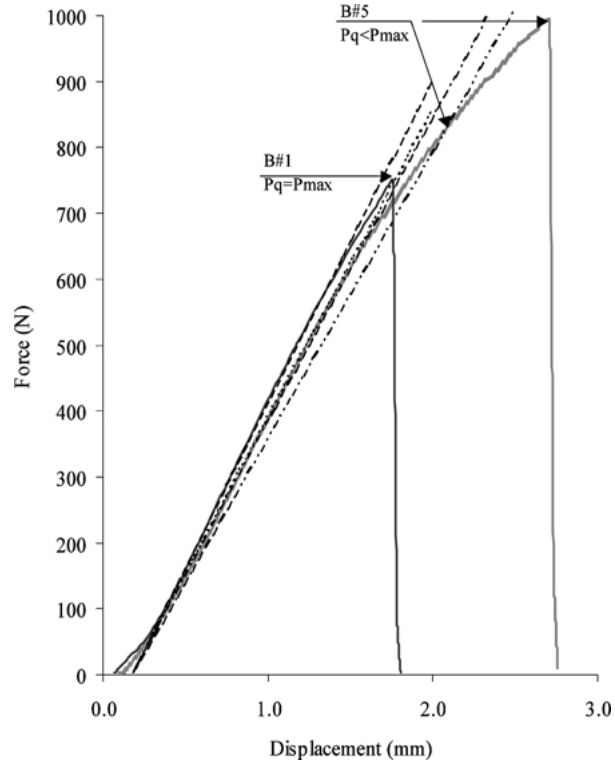

Figure 18 Comparison of force – displacement traces from fracture toughness testing for acetal blends B#1 and B#5.

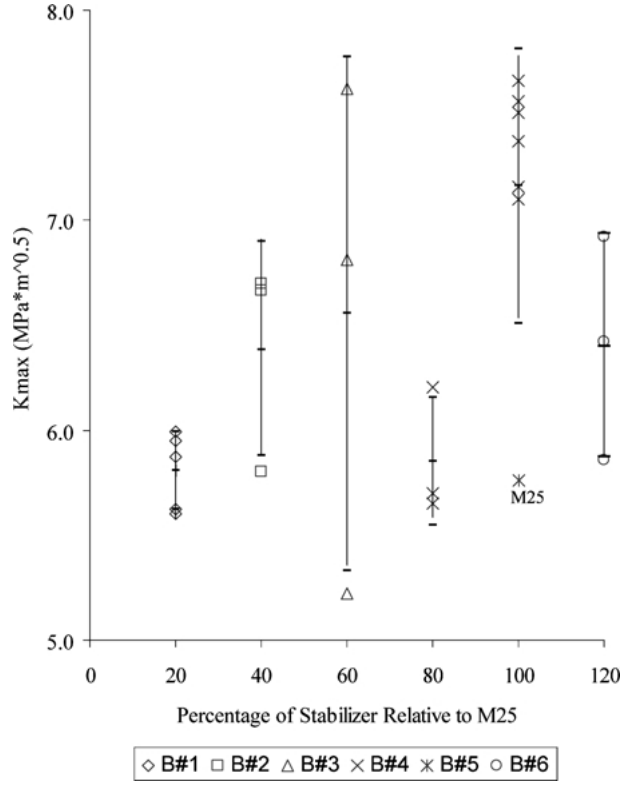

Figure 19 Fracture toughnesses for acetal blends calculated using maximum loads. Mean values and standard deviations are shown.

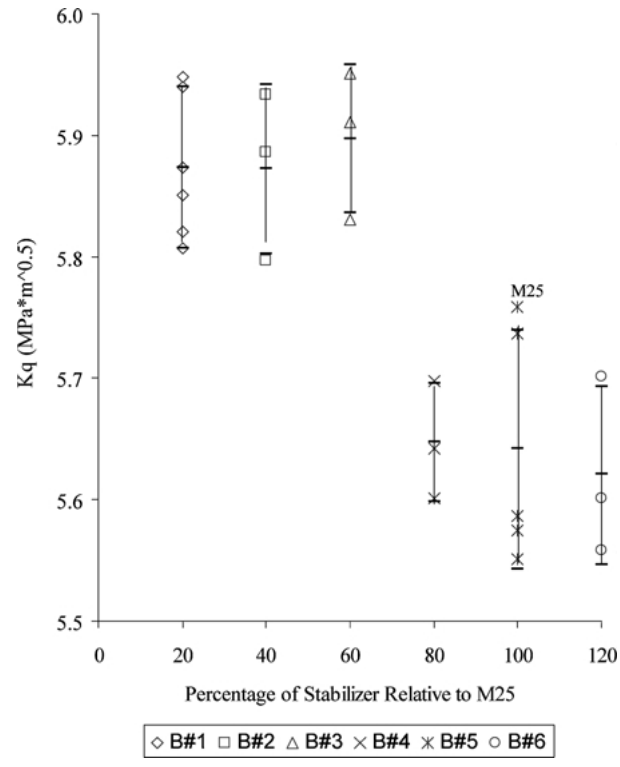

Figure 20 Fracture toughnesses for acetal blends calculated using offset loads, P_Q.

and in fact in Fig. 19 one can see that significant scatter exists for the calculated fracture toughnesses from P_M values versus percentage of stabilizer.

Fracture toughnesses were also calculated using the relative values of P_Q to compare the blends. This is shown in Fig. 20. The results indicate that a relatively constant value of K_Q of 5.9 MPa*m$^{0.5}$ is observed for blends B#1–B#3 with a decreased level of 5.7 MPa*m$^{0.5}$ for the blends B#4–B#6. These results, although clearly differentiating the blends, suggests that the higher concentration of stabilizer leads to a lower fracture toughness. This false conclusion relates to the invalid nature of the K_{1c} measurement for the blends

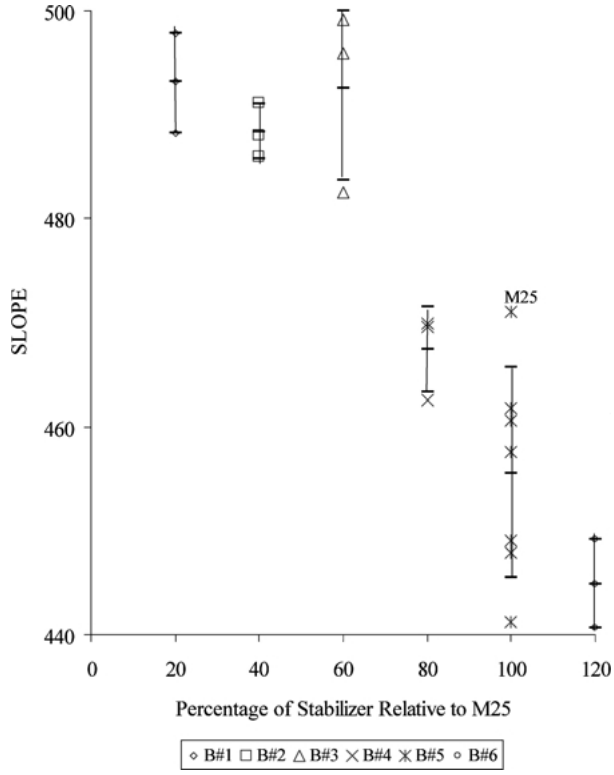

Figure 21 Slopes of the load – displacement traces during fracture toughness testing of acetal blends.

of higher stabilizer concentration. The latter would be expected to provide higher values of fracture toughness if for example thicker samples were available to perform the measurements. In spite of the apparent contradiction in toughness, the behavior of the blends clearly distinguishes the effect of stabilizer concentration. Similarly the initial slope of the load-displacement curve during the K_{1c} test also distinguishes blends B#1–B#3 from the higher levels of stabilizer. This is shown in Fig. 21. Of course the slope values presumably reflect the higher moduli for the blends with lower stabilizer contents as already shown in Fig. 15. However, the data shown in Fig. 21 suggest a more precipitous decrease in slope as stabilizer content increases which may reflect the contribution of localized ductility as well as stiffness in this particular experiment using precracked specimens.

It is interesting to compare the physical observations of crack initiation and growth with the mechanical data. During the fracture toughness tests, the sequence of events is as follows: the precrack gradually opens, a plastic zone initiates at the crack tip, the crack tip extends into the plastic zone. The latter can occur catastrophically or in a stable slow crack growth mode. For the slow crack growth mode, both the crack tip and plastic zone appear to propagate together up to the point of instability where catastrophic rupture occurs. The initial straight line portion of the load -displacement curve reflects both crack opening and plastic zone development, but not crack growth. Crack growth does occur in a stable fashion even before the load, P_Q, thus the crack lengths for K_Q calculations were taken from the fracture surfaces, not initial precrack lengths. For this reason, P_Q values alone cannot be used to assess the calculated K_Q values. The observations of the crack tip plastic zone development also suggest that it is the stability of this zone, or ability to sustain load, which controls the ultimate fracture toughness of the acetal materials.

3.6. Effect of room temperature aging

As mentioned earlier, the material was supplied in the form of pellets which were immediately injection molded into test plaques. However, after some preliminary fatigue measurements, referred to here as "old" tests, the project was put on hold for about two years when most of the measurements were made for this study. Thus the plaques had in effect been aged at room temperature. It was therefore of interest to compare both old and new fatigue testing results to establish any effect of this storage at room temperature.

Figs 22 and 23 show the effect of aging on FCP results for two blends (B#1 & M25). Note that both tests (the old and the new) were conducted under identical conditions (similar load, notching, temperature, frequency, and specimen dimensions). Fig. 22 shows the effect of aging on sample M25, the commercial acetal material. It is clear from this figure that aging for three years increases the crack propagation rate by a factor of two at the initial stress intensity factor (ΔK_i). In contrast, Fig. 23 shows the effect of the aging process on B#1 which had only 20% stabilizer relative to M25. As expected,the lower stabilizer content in the material leads to more degradation and this is reflected in the accelerated fatigue crack propagation rates after aging. The crack speed at the initial stress intensity factor (ΔK_i) is two orders of magnitude higher (faster) for the aged sample. Specifically, after two to three years of storage

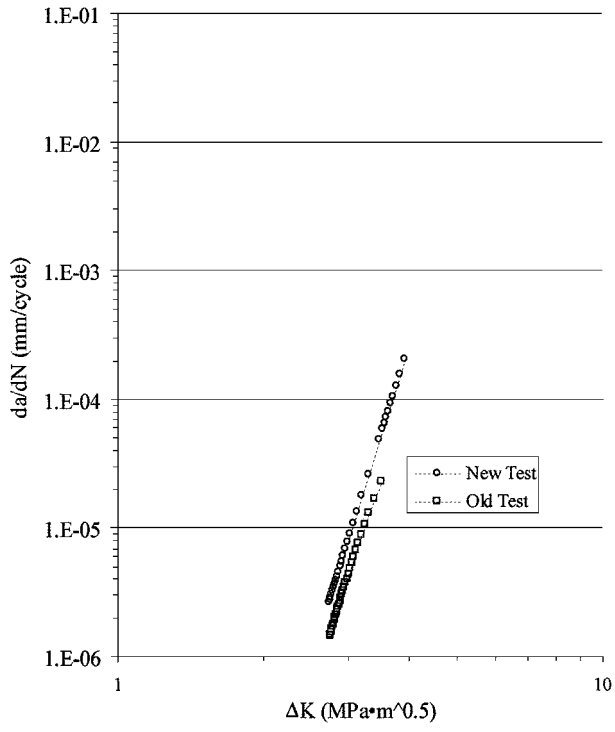

Figure 22 Effect of room temperature aging on fatigue crack growth rates for Celcon M-25.

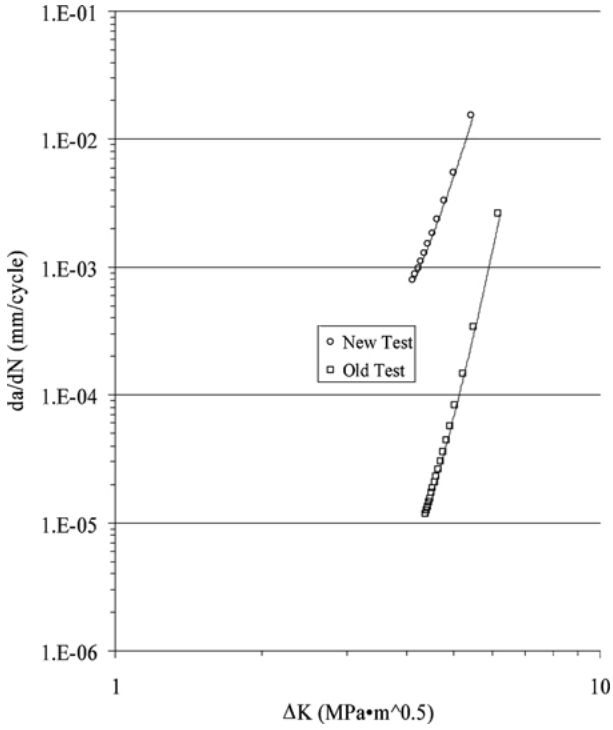

Figure 23 Effect of room temperature aging on fatigue crack growth rates for blend B#1.

at room temperature the fatigue crack growth rate is increased by a factor of 170.

Since aging often is associated with a decrease in molecular weight an attempt was made to measure the difference between molecular weights for all of the acetal blends by using gel permeation chromatography, GPC. Fortunately the GPC measurements had also been run prior to the long term room temperature storage which allowed this comparison. However the results of both weight average, Mw, and number average, Mn, molecular weight determinations showed no significant changes for these blends and any differences between the various blends were also negligible. Whether this is attributed to interpretation or uncertainty of the GPC results, or reflects the subtle changes needed to influence fatigue behavior is not clear.

4. Summary and conclusions

This research was complicated by the difficulty in obtaining stable fatigue crack propagation rate measurements for the acetal materials; the indications of different mechanisms for stable fatigue crack growth at low versus high ΔK levels; and the similarity of all of the crack growth rate data for the blends at low ΔK levels. The fact that the da/dN curves do not shift significantly, but rather exhibit differing slopes, puts an added burden on the accuracy of the data analysis and measurement procedure. By combining the usual Paris plot with the additional method [5] for plotting crack length versus number of cycles, it is believed that a valid interpretation has been achieved. Both the assessment of fatigue resistance and the determination of short term mechanical properties demonstrate the influence of stabilizer concentration on the performance of injection molded acetal material. In addition, there are indications that a critical level of stabilizer exists and that even higher levels may continue to provide benefit. Furthermore, the fatigue crack propagation rate data indicates that the relatively small temperature increase from 25°C to 60°C has a profound effect on the calculated fatigue lifetimes. The decrease in fatigue life at higher temperatures is not unexpected based on previous observations for a variety of polymers [20] as well as data for nylon materials taken in our laboratories. However, in view of the possible role of crack initiation it would be valuable to replicate these results by testing uncracked specimens before firm conclusions are drawn. Taken together, all of the results of this study suggest that relatively strict control of the processing history as well as the initial chemistry of the acetal is important in order to insure the uniformity of the long term durability of molded acetal products.

Acknowledgement

The authors wish to thank Glen Novak and John Krohn of the Delphi Automotive Systems Research Labs Polymer's Group for assistance in sample preparation, testing and setting up equipment as well as many helpful discussions. Acetal blends were kindly provided by Randall Hanes and Steve Sinker of Ticona.

References

1. H. F. MARK, N. M. BIKALES, C. G. OVERBERGER and G. MENGES, "Encyclopedia of Polymer Science and Engineering," 2nd ed. (Wiley, Interscience, 1985) Vol. 1, p. 42.
2. F. R. STOHLER and K. BERGER, *Die Angewandte Chemie* **176/177** (1990) 323.
3. R. W. HERTZBERG, M. D. SKIBO and J. A. MANSON, *J. Mater. Sci.* **13** (1978) 1038.
4. A. LAZZERI, A. MARCHETTI and G. LEVITA, *Fatigue and Fracture of Engineering Materials and Structure* **20**(8) (1997) 1207.
5. A. J. LESSER, *J. Appl. Polym. Sci.* **58** (1995) 869.
6. R. CONNOLY and R. GAUVIN, *Polymer Engineering and Science* **25** (1985) 548.
7. R. VINET, R. CONNOLY and R. GAUVIN, *ibid.* **21** (1981) 1203.
8. P. BRETZ, R. W. HERTZBERG and J. A. MANSON, *J. Appl. Polym. Sci* **27** (1982) 1707.
9. A. J. LESSER, *Polymer Engineering and Science* **36** (1996) 2366.
10. J. PECORINI, R. W. HERTZBERG and J. A. MANSON, *J. Mater. Sci.* **25** (1990) 3385.
11. M. G. WYZGOSKI and G. E. NOVAK, *J. Mater. Sci.* **25** (1990) 4501.
12. X. WANG, K. SEHANOBISH and A. MOET, *Polymer Composites* **9** (1968)165.
13. E. A. SHOWAIB and A. MOET, *J. Mater. Sci.* **28** (1993) 3617.
14. E. A. SHOWAIB, K. SEHANOBISH and A. MOET, *Polymer Engineering and Science* **35**(9) (1995) 786.
15. J. KREY, K. FRIEDRICH and A. MOET, *Polymer* **29** (1988) 1433.
16. K. SEHANOBISH, A. MOET and A. CHUDNOVSKY, *ibid.* **28** (1987) 1315.
17. P. PARIS and F. ERDOGAN, *Transactions of the ASME* **85**(4) (1963) 528.
18. H. TADA, P. C. PARIS and G. R. IRWIN, "The Stress Analysis of Cracks Handbook" (Del Research Corp., St. Louis, MO, 1985).
19. Y. Q. ZHOU and N. BROWN, *J. Polym. Sci.* B **30** (1992) 477.
20. R. W. HERTZBERG and J. A. MANSON, "Fatigue of Engineering Plastics" (Academic Press, San Diego, CA, 1980) p. 106.

Received 7 September 2000
and accepted 29 November 2001